# The Effect of Alkaline Earth (Ba, Sr and Ca) Doped Iron Bismuth Glasses on The Structural, Thermoelectric and Electrical Properties

**Ahmed Hannora** ( ahmed.hannora@suezuniv.edu.eg )
Suez University
**A. M. Ali**
Suez University
**E. El-Falaky**
Suez University
**M. M. El-Desoky**
Suez University

**Research Article**

**Keywords:** Iron bismuth glasses, XRD, DSC, thermoelectric power; and dc conductivity, SPH

**Posted Date:** May 28th, 2021

**DOI:** https://doi.org/10.21203/rs.3.rs-557850/v1



**Version of Record:** A version of this preprint was published at Journal of Inorganic and Organometallic Polymers and Materials on November 22nd, 2021. See the published version at https://doi.org/10.1007/s10904-021-02141-8.

# The effect of alkaline earth (Ba, Sr and Ca) Doped Iron Bismuth glasses on the Structural, thermoelectric and electrical properties

***Ahmed E. Hannora [a], A. M. Ali [b], E. El-Falaky [b], M. M. El-Desoky [b]***

*[a] Department of Science and Mathematical Engineering, Faculty of Petroleum and Mining Engineering, Suez University, Suez, Egypt, 43721.*

*[b] Department of Physics, Faculty of Science, Suez University, Suez, Egypt.*

## Abstract

Glasses with nominal composition $70Bi_2O_3$-$30Fe_2O_3$ and 10A-$60Bi_2O_3$-$30Fe_2O_3$ (mol%); (A=Ba, Sr and Ca) were prepared by the conventional melt quenching technique. X-ray diffraction (XRD) and Differential scanning calorimeter (DSC) confirm the amorphous nature of the glass samples. The iron-bismuth glasses show good solubility of alkaline earth elements ions. In temperatures range of 310 - 450 K, the dc conductivity of the glass samples containing alkaline earth elements enhanced. Glass sample containing Sr shows interesting electrical properties. All glass samples showed a transition from negative to positive Seebeck coefficient, this means that the conduction is mixed of electrons and holes charge carriers. The conduction mechanism of all samples obeys non-adiabatic small polaron hopping model of electron between iron ions. The calculated small polaron coupling constant, ($\gamma_p$) was found to be in the range of 10.25–17.28. Also, the calculated hopping mobility ($\mu$) and carrier density ($N_c$) of glasses were in the range of $4.65\times 10^{-7}$- $4.11\times 10^{-3}(\mathrm{cm^2V^{-1}s^{-1}})$ and 0.029-10 ($\times 10^{17}\mathrm{cm^{-3}}$) at 333 K, respectively.

**Keywords:** Iron bismuth glasses**;** XRD; DSC; thermoelectric power; and dc conductivity; SPH

## 1. Introduction

Recently multicomponent oxide glasses containing transition and/or heavy metal oxides attracted a considerable attention due to its possible applications. Among the heavy metal oxides, $Bi_2O_3$ has attracted much attention because of its high optical properties such as density, IR transmission and polarizability so $Bi_2O_3$ is used as layers for optoelectronic devices [1, 2]. Transition metal ions addition such as (Fe) to glasses lead to interesting electrical properties with promising technological applications in electronic and optical devices [3]. The addition of $Fe_2O_3$ to the bismuth glasses is expected to get better electrical properties The electrical conductivity mechanism of iron-bismuth glasses was studied by several authors [4-6] which described by the small polaron hopping (SPH) model between ions present in different valance states where electron hopping from low $Fe^{2+}$ to high valance $Fe^{3+}$ sites [7, 8]. The electrical conductivity strongly depends locally upon the interaction of an electron with its surroundings and the distance between the Fe-ions [9].

The glasses with ionic conductivity attract much scientific attention because of their potential applications such as solid-state batteries, memory devices and sensors [10]. Recently, M.G. Moustafa et. al [3], studied the electrical transport properties of iron bismuth glasses and revealed that, $Fe_2O_3$ played a significant role in the electrical conduction enhancement. $Bi_2O_3$-$Fe_2O_3$ glasses containing alkaline earth elecments conductivity consist of ionic and electronic conduction. Ideally, the motion of alkaline earth ions and electrons are not dependent of each other [11, 12]. Shangjie Chu [13], investigated the effect of the alkaline earth elements addition on the electrical conduction for $Bi_{0.9}A_{0.1}FeO_3$ (A=Ca, Sr and Ba) ceramics synthesized by solid state reaction method. The substitution of alkaline earth elements like Ba, Sr and Ca have a great impact on structural, thermoelectric and electrical properties of iron-bismuth glasses [14].

In this work, glasses of $70Bi_2O_3$-$30Fe_2O_3$ are synthesized by using the conventional melt quenching technique. The effect of alkaline earth (Ba, Sr and Ca) doped iron bismuth glasses on the structural, thermoelectrical and electrical properties were investigated.

## 2. Experimental

Glasses of $70Bi_2O_3$-$30Fe_2O_3$ and 10A-$60Bi_2O_3$-$30Fe_2O_3$ (mol%); (A=Ba, Sr and Ca) were prepared by the conventional melt quenching technique from reagent grade $Bi_2O_3$ (99 % , Loba Chemie), $Fe_2O_3$ (99.9 %), $BaCO_3$ (99% , Koch-Light Laboratory Ltd), SrO (99.9% , Sigma Aldrich) and $CaCO_3$ (99% , Koch-Light Laboratory Ltd). They are designated as BBFO, BSFO and BCFO for the corresponding Ba, Sr and Ca doped BFO ($Bi_2O_3$-$Fe_2O_3$) glass samples, respectively. The powder mix-up was heated in a platinum crucible for 30-40 minutes to insure complete homogeneity in electric furnace at 900-1280 ºC. After casting in stainless steel mold, the melt quickly pressed by another thick stainless-steel plate at room temperature to obtain around 2.0 mm in thickness opaque glasses.

The amorphous nature of the glasses was checked by Siemens D5000 X-ray diffractometer with nickel-filtered Cu $K_\alpha$ radiation under accelerating voltage of 40 kV and current of 30 mA. The collected diffraction data was over a 2θ range of 5° to 60° at a scan rate of 3 degree per second. Thermal analysis was performed in the temperature range from room temperature to 850 K using differential scanning calorimetry NETZSCH DSC 204, with heating rate 10 K/min. The glass samples densities (ρ) were measured at room temperature by Archimedes method using Toluene as the immersion liquid, the measurement was performed 3 times.

Glass samples were grinded and polished with emery paper to obtain parallel surfaces of ~ 1.5 mm thickness. Silver paste electrodes deposited on both faces of the polished samples. The DC conductivity of the glass samples was measured at temperatures between 310 and 450 K using Picoammeter type KEITHLEY 485. Hewlett Packard 34401A multimeter in temperature range 300-480 K was used for thermoelectric power measurements.

## 3. Results and discussion

Fig. 1 shows the X-ray diffraction (XRD) patterns of the $70Bi_2O_3$-$30Fe_2O_3$ and 10A-$60Bi_2O_3$-$30Fe_2O_3$ (mol%); (A=Ba, Sr and Ca) glass samples. It is observed that the quenched samples exhibit broad humps without any crystalline peaks which indicate the amorphous nature of the glass samples. Fig. 2 shows, differential scanning calorimetry (DSC) curve of BFO sample with glass transition temperature ($T_g$) at 742 K followed by two exothermic crystallization peaks $T_{C1}$ = 770 K and $T_{C2}$ = 805 K. The thermal stability factor ($\Delta T = T_{C2} - T_g$) usually employed to estimate the glass stability. The approximately large $\Delta T$ value (63 K) estimated from DSC data indicates high thermal stability of this glass.

The densities of the glass samples were measured by Archimedes method using the following equation [15, 16]:

$$\rho = \rho_L \times \frac{W_a}{W_a - W_L} \quad (1)$$

where $W_a$ is the quenched glass sample weight in air, $W_L$ was the glass sample weight in Toluene and $\rho_L$ was the Toluene density at room temperature, which was 0.866 g/cm$^3$.The molar volume $V_m$ of the glass samples can be calculated according to the following equation [16]:

$$V_m = \frac{M}{\rho} \quad (2)$$

where M is the total molecular weight and ρ is the glass sample calculated density. The densities of the glass samples increased in the order of BCFO<BSFO<BBFO<BFO, with increasing molar weight of the alkaline-earth ions while molar volume shows opposite behavior, Fig. 3 and Table 1.

### 3.1. Seebeck Coefficient Measurement

By measuring the thermoelectric power, Seebeck coefficient (S) was estimated when a temperature gradient was applied to both sides of the glass samples. The equation was described as $S = \Delta V/\Delta T$, where the major charge carrier becomes holes for a positive (+) S and the major charge carrier becomes electrons for a negative (-) S [17].

From Fig. 4, all glass samples showed a transition from negative to positive Seebeck coefficient " S ", this means that the conduction is mixed of electrons and holes charge carriers. Thermoelectric power measurements were used to determine the fraction of reduced transition metal ion ratio, $C = Fe^{2+}/Fe_{total}$ ,by the methods described by Heikes et al [18, 19]. It has been demonstrated that the Seebeck coefficient and obeys the following relationship which depends on the ratio of high to low valence state of iron [18, 19]:

$$S = \frac{K}{e} \ln\left(\frac{c}{1-c}\right) = \frac{K}{e} \ln\left(\frac{Fe^{2+}}{Fe^{3+}}\right) \quad (3)$$

Table 1 shows the C values for the present glass samples which estimated by using S.

### 3.2. Dc electrical conductivity

#### 3.2.1. Conductivity and activation energy

Fig. 5 shows the variations of DC conductivity (σ) of glass samples as a function of reciprocal of the absolute temperature (T). It is clearly seen that a linear temperature dependence up to a certain temperature $\theta_D/2$ ($\theta_D$: Debye temperature). The activation energy (W) is temperature dependent and can be calculated from the slope of the linear fitting of the conductivity curve at higher temperature according to the following formula:

$$\sigma = \sigma_o \exp(-W/k_BT) \quad (4)$$

where $\sigma_o$ is the pre-exponential factor, $k_B$ is the constant of Boltzmann's and T is the absolute temperature. It is observed that σ smoothly increases with temperature, indicating a semiconducting nature of glass samples. The DC conductivity of the alkaline earth added glasses is always higher than that of bismuth-iron glasses with higher conductivity value for BSFO sample.

Fig. 6 illustrates the DC conductivity and activation energy variation as a function of alkaline earth metals. A general trend observed in this figure, is that the conductivity at fixed temperature (333 K) tends to be increased with alkaline earth elements addition and the maximum value observed with sample containing strontium while the opposite trend can be observed for the activation energy values. Such behavior arises from the polarons hopping or electrons between mixed valance states [11, 12, 20]. The experimental conductivity data above $\theta_D/2$ were fitted with SPH model proposed by Mott [21]. The activation energy values are found to be 0.562 eV, 0.355 eV and 0.569 eV for BAFO (A = Ca, Sr and Ba) glass samples, respectively. The enhancement of conductivity and activation energy reduction agree with transition metal ion ratio values calculated from thermoelectric power measurements. The ionic conduction of the added alkaline earth elements could play a significant role in conductivity enhancement.

#### 3.2.2 Nature of conduction mechanism

The hopping conductivity in (TM) oxide glasses was investigated by Mott [21]. Due to the strong interaction between electrons and optical phonons, small polaron created at enough higher temperatures [22]. In non-adiabatic hopping regime, where the electron has a low opportunity of making the transfer during each excitation the DC conductivity of the nearest neighbor hopping at high temperatures $T > \theta_D/2$ is expressed as the following by

$$\sigma = \upsilon_o Ne^2R^2C (1-C) \exp(-2\alpha R) \exp(-W/k_BT) \quad (5)$$

where $\upsilon_o$ is the optical phonon frequency which measured from the electrical conductivity data according to the relation ($k_B \theta_D = h \upsilon_o$) the values of $\upsilon_o$ are listed in Table. 1, α is the tunneling factor, N is the density of transition metal ion, R is the mean distance between Fe ions, e is the electronic charge and C is the fraction of reduced Fe ion ($C = Fe^{2+}/\Sigma Fe$),

The pre-exponential factor $\sigma_o$ in Eq. 4 can be expressed as

$$\sigma_o = \upsilon_o \, Ne^2R^2C \, (1\text{-}C) \exp(-2\alpha R) \tag{6}$$

According to Austin and Mott [23] model for strong electron–phonon interaction, the hopping conduction activation energy is given by;

$$W = W_H + \frac{W_D}{2} \quad \text{for } T > \theta_D/2 \tag{7}$$

$$W = W_D \quad \text{for } T > \theta_D/4 \tag{8}$$

Where $W_H$ (=Wp/2) is the hopping energy and $W_D$ is the disorder energy which defined as the difference of electronic energies between two hopping sites $Fe^{+2} \leftrightarrow Fe^{+3}$.

$$W_D = (e^2/\varepsilon_o\varepsilon_s \, R) \, L \tag{9}$$

Where $\varepsilon_s$ is the static dielectric constant and *L* is a constant of factor 0.3. The values of $W_D$ were calculated found to be in the range of 0.11-0.25 eV.

In the adiabatic hopping regime, the electron makes transitions backward and forward several times during excitation between hopping sites $Fe^{+2} \leftrightarrow Fe^{+3}$. In this case αR in Eqs. 5 and 6 becomes negligible [21-23], then the σ and the $\sigma_o$ in Eqs. 5 and 6 were expressed as the following:

$$\sigma = \upsilon_o \, N \, e^2 \, R^2 \, C \, (1\text{-}C) \exp \, (-W/k_BT) \tag{10}$$

and

$$\sigma_o = \upsilon_o \, N \, e^2 \, R^2 \, C \, (1\text{-}C) \tag{11}$$

The of polaron hopping mechanism nature (adiabatic or non-adiabatic) can be obtained from a plot of ln $\sigma$ against activation energy W at fixed experimental temperature T. If the temperature estimated $T_e$, from the slope of such a plot is close to experimental temperature T, the hopping conduction will be in the adiabatic regime. Otherwise it is expected that the hopping will be in the non-adiabatic regime.

Fig. 7 shows the relationship between lnσ versus W for all glass samples at fixed temperature (333K). The estimated temperature ($T_e$ = 247 K) calculated from the slope of the plot is differ than the temperature chosen (T = 333 K) confirming that the conduction mechanism in the present glass samples is due to non-adiabatic SPH of electrons [3].

### 3.2.3 Activation energy and mean distance between Fe ions relation

The concentration of Fe ions per unit volume, N ($cm^{-3}$) in the glass samples was calculated using the density by the relation [24]

$$N = 2 \, N_A \left(\frac{F_W \, \rho}{M_W}\right) \tag{12}$$

where $N_A$ is the Avogadro number, $F_w$ is the weight fraction of $Fe_2O_3$ and $M_w$ is the molecular weight of $Fe_2O_3$ and ρ is the density of the sample. The mean distance R between Fe ions in the glass samples was calculated from

$$R = \left(\frac{1}{N}\right)^{\frac{1}{3}} \quad (13)$$

The values of R and N are given in Table 1.

### 3.2.4 Nature of small polaron hopping (SPH) conduction

In small polaron hopping (SPH) conduction, the polaron bandwidth (J) obeys [25]:

$$J > \left(\frac{2kTW_H}{\pi}\right)^{\frac{1}{4}} \left(\frac{\hbar\upsilon_o}{\pi}\right)^{\frac{1}{2}} \quad \text{(adiabatic)} \quad (14)$$

$$J < \left(\frac{2kTW_H}{\pi}\right)^{\frac{1}{4}} \left(\frac{\hbar\upsilon_o}{\pi}\right)^{\frac{1}{2}} \quad \text{(non-adiabatic)} \quad (15)$$

The limiting values of (J) calculated from the right-hand side of the equation (14) or (15) at fixed temperature (333K) is in the range of 0.015 – 0.018 eV depending on sample composition. Therefore, the condition for the existence of (SPH) is content dependance.

For adiabatic hopping conduction, $W_H$, is given using J as

$$W - W_D/2 \simeq W_H = W_p/2 = W`_p/2 - J \quad (16)$$

Where $W_p$ is the polaron binding energy, $W`_p$ is the maximum polaron binding energy and $W_H$ depends on R [26].

Otherwise, for non-adiabatic hopping conduction, $W_H$, is given by

$$W - W_D/2 \simeq W_H = W`_p/2 \quad (17)$$

Using the values of $W_D$ and W, we obtained $W_H$ in the order of (0.30-0.55) eV. These values are close to W values for the present glass samples.

Next, by using the mean spacing between the Fe-ions, R, in Table. 1, the polaron radius ($r_p$) is given by relation:

$$r_p = \frac{R}{2}\left(\frac{\pi}{6}\right)^{\frac{1}{3}} \quad (18)$$

The values of R and $r_p$ are described in Tables 1 and 2.

$N(E_F)$ is the density of states at Fermi level can be estimated in term of W as [27, 28].

$$N(E_F) = \left(\frac{3}{4\pi R^3 W}\right) \quad (19)$$

The values of $N(E_F)$ for the present glass samples are listed in Table 2. It is clear that, the density of states $N(E_F)$ is the order of $10^{21}$ ($eV^{-1}cm^{-3}$). The values of $N(E_F)$ are reasonable for the localized states [27, 29].

The small polaron coupling constant $\gamma_p$, is representing the electron-phonon interaction. The values of ($\gamma_p$) given by

$$\gamma_p = \frac{2\,W_H}{h\,\upsilon_o} \tag{20}$$

were also calculated for the glass samples[7]. The evaluated values of $\gamma_p$ are listed in Table. 2. The values of $\gamma_p > 4$ for all glass samples usually indicate a strong electron–phonon interaction [29]. From results listed in Table 2, we can deduce that the $\gamma_p$ has minimum value at the highest conductivity sample (BSFO).

The hopping carrier mobility $\mu$ in the non-adiabatic hopping mechanism is given by the following equation[23] .

$$\mu = \left(\frac{eR^2}{kT}\right)\left(\frac{1}{\hbar}\right)\left(\frac{\pi}{4W_H kT}\right)^{\frac{1}{2}} J^2 \exp\left(-\frac{W}{kT}\right) \tag{21}$$

Also, the carrier density *($N_c$)* values was calculated from the relation[30] .

$$\sigma = N_c\, e\, \mu \tag{22}$$

The values of $\mu$ and $N_c$ for the glass samples at 333 K are listed in Table. 3. Because the localization condition for hopping electrons is $\mu < 0.01$ ($cm^2V^{-1}s^{-1}$) [22, 28, 31] , the results show that electrons in the present glass samples are localized at the Fe-ion sites. Also the constant $N_c \sim 10^{17}$ indicates that the conductivity of glass samples is determined by hopping mobility[27].

We will now apply the law suggested by Greaves [32] as a modification of Mott's variable range hopping (VRH) model [23], Greaves's VRH model could be applied at intermediate temperature (below $\theta_D/2$). The expression for the DC conductivity ($\sigma$) according to Greaves's VRH model is given by formula:

$$\sigma\, T^{\frac{1}{2}} = A \exp\left(\frac{-B}{T^{\frac{1}{4}}}\right) \tag{23}$$

where A and B are constants and B is given by

$$B = 2.1\left(\frac{\alpha^3}{k_B\, N(E_F)}\right)^{\frac{1}{4}} \tag{24}$$

Fig. 8 shows the plot of $\ln(\sigma T^{1/2})$ versus $T^{-1/4}$. A good fit of the experimental data to formula (23) in the intermediate temperature range, suggesting that Greave's VRH may be valid in this glass samples over the entire temperature range. Table 4 shows the values of parameters A and B from these curves. In addition, we can apply formula (24) to calculate the factor $\alpha$. The values of $\alpha$ and $N(E_F)$ are reasonable for the localized states [23, 33].

## 4. Conclusion

Glasses of $70Bi_2O_3$-$30Fe_2O_3$ and 10A-$60Bi_2O_3$-$30Fe_2O_3$ (mol%); (A=Ba, Sr and Ca) were prepared by the conventional melt quenching technique. From the XRD results all the glass samples were fully amorphous in nature. Density ($\rho$) was found to increase with decreasing the molar volume ($V_m$). Dc conductivity increased with the addition of alkaline earth elements with BSFO maximum value. The conductivity enhancement and activation energy reduction agree with transition metal ion ratio values calculated from thermoelectric power measurements. The DC electrical conductivity in the glass samples was due to non-adiabatic small polaron hopping (SPH) model of electron between Fe-ions. The electron–phonon interaction coefficient, ($\gamma_p$) was calculated and found to be in the range of 10.25–17.28. The nearly constant of carrier density (Nc) ~ $10^{17}$ $cm^{-3}$ indicates that the conductivity is determined by the hopping mobility.

## References


[1] C. Tripon, D. Toloman, M. Aluas, C. Filip, I. Ardelean, Structural investigation of the xV2O5 (1-x)[Bi 2O3-B2O3] glasses by IR absorbtion, EPR and NMR, Journal of Optoelectronics Advanced Materials 8(3) (2006) 1129.

[2] S.R. Pelluri, R. Singh, ESR and magnetization studies of Fe2O3–Bi2O3–ZnO–PbO glass system, Journal of magnetism Magnetic Materials 418 (2016) 206-212.

[3] M. Moustafa, Electrical transport properties and conduction mechanisms of semiconducting iron bismuth glasses, Ceramics International 42(15) (2016) 17723-17730.

[4] H. Qiu, T. Ito, H. Sakata, DC conductivity of Fe2O3–Bi2O3–B2O3 glasses, Materials chemistry physics of the Solid State 58(3) (1999) 243-248.

[5] A. Al-Hajry, N. Tashtoush, M. El-Desoky, Characterization and transport properties of semiconducting Fe2O3–Bi2O3–Na2B4O7 glasses, J Physica B: Condensed Matter 368(1-4) (2005) 51-57.

[6] M.S. Dahiya, A. Yadav, N. Manyani, S. Chahal, A. Hooda, A. Agarwal, S.J.J.o.T.A. Khasa, Calorimetry, Fe-substituted Co-Li bismuth borate glasses, 126(3) (2016) 1191-1199.

[7] N. Mott, Conduction in glasses containing transition metal ions, Journal of Non-Crystalline Solids 1(1) (1968) 1-17.

[8] L. Murawski, Electrical conductivity in iron-containing oxide glasses, Journal of materials science. Materials in medicine 17(8) (1982) 2155-2163.

[9] M.M. El-Desoky, M.M. Mostafa, M.S. Ayoub, M.A. Ahmed, Transport properties of Ba-doped BiFeO3 multiferroic nanoparticles, Journal of Materials Science: Materials in Electronics 26(9) (2015) 6793-6800.

[10] A. Agarwal, V. Seth, P. Gahlot, S. Khasa, P. Chand, Effect of Bi2O3 on EPR, optical transmission and DC conductivity of vanadyl doped alkali bismuth borate glasses, Journal of Physics and Chemistry of Solids 64(11) (2003) 2281-2288.

[11] A. Al-Shahrani, M. El-Desoky, Electrical transport studies in alkali iron phosphate glasses, Journal of Materials Science: Materials in Electronics 17(1) (2006) 43-49.

[12] M. El-Desoky, A. Al-Shahrani, Mixed electronic–ionic conductivity in semiconducting CaO–PbO–Fe2O3–P2O5 glasses, Physica B: Condensed Matter 371(1) (2006) 95-99.

[13] S. Chu, M. Zhang, H. Deng, Z. Wang, Y. Wang, Y. Pan, H. Yan, Investigation of doping effect on electrical leakage behavior of BiFeO3 ceramics, Journal of Alloys Compounds 689 (2016) 475-480.

[14] S. Chauhan, M. Kumar, S. Katyal, Band-gap tuning and magnetic properties of heterovalent ions (Ba, Sr and Ca) substituted BiFeO3 nanoparticles, AIP Conference Proceedings, AIP Publishing LLC, 2016, p. 130029.

[15] A.E. Hannora, M. El-Desoky, Effects of heat treatment on the structural and electrical conductivity of Fe 2 O 3–P 2 O 5–PbO glasses, Journal of Materials Science: Materials in Electronics 30(21) (2019) 19100-19107.

[16] K. Kirdsiri, R.R. Ramakrishna, B. Damdee, H. Kim, S. Kaewjaeng, S. Kothan, J. Kaewkhao, Investigations of optical and luminescence features of Sm3+ doped Li2O-MO-B2O3 (M= Mg/Ca/Sr/Ba) glasses mixed with different modifier oxides as an orange light emitting phosphor for WLED's, Journal of Alloys Compounds 749 (2018) 197-204.

[17] J.W. Woo, S. Baek, T.K. Song, M.H. Lee, J.U. Rahman, W.-J. Kim, Y.S. Sung, M.-H. Kim, S. Lee, J.W. Woo, Nonstoichiometric effects in the leakage current and electrical properties of bismuth ferrite ceramics, Journal of the Korean Ceramic Society 54(4) (2017) 323-330.

[18] R. Heikes, Thermoelectricity ed RR Heikes and RW Ure, New York: Interscience1961.

[19] M. El-Desoky, M. Al-Assiri, A. Bahgat, Structural and thermoelectric power properties of Na-doped V2O5· nH2O nanocrystalline thin films, Journal of Physics Chemistry of Solids 75(8) (2014) 992-997.

[20] M. El-Desoky, A. Al-Hajry, M. Tokunaga, T. Nishida, M. Hassaan, Effect of sulfur addition on the redox state of iron in iron phosphate glasses, Hyperfine Interactions 156(1-4) (2004) 547-553.

[21] N.F. Mott, Conduction in non-crystalline materials: III. Localized states in a pseudogap and near extremities of conduction and valence bands, Philosophical Magazine 19(160) (1969) 835-852.

[22] M. El-Desoky, M. Mostafa, M. Ayoub, M. Ahmed, Transport properties of Ba-doped BiFeO3 multiferroic nanoparticles, Journal of Materials Science: Materials in Electronics 26(9) (2015) 6793-6800.

[23] I. Austin, N.F. Mott, Polarons in crystalline and non-crystalline materials, Advances in physics 18(71) (1969) 41-102.

[24] M. Pant, D. Kanchan, P. Sharma, M.S. Jayswal, Mixed conductivity studies in silver oxide based barium vanado–tellurite glasses, Materials Science Engineering: B 149(1) (2008) 18-25.

[25] M. Al-Assiri, S. Salem, M. El-Desoky, Effect of iron doping on the characterization and transport properties of calcium phosphate glassy semiconductors, Journal of Physics Chemistry of Solids 67(8) (2006) 1873-1881.

[26] H. HIRASHIMA, D. ARAI, T. YOSHIDA, Electrical Conductivity of PbO-P2O5-V2O5Glasses, Journal of the American Ceramic Society 68(9) (1985) 486-489.

[27] M. El-Desoky, Small polaron transport in V2O5–NiO–TeO2 glasses, Journal of Materials Science: Materials in Electronics 14(4) (2003) 215-221.

[28] N.F. Mott, E.A. Davis, Electronic processes in non-crystalline materials, Oxford university press2012.

[29] M. El-Desoky, I. Kashif, Electrical conductivity in mixed calcium and barium iron phosphate glasses, physica status solidi 194(1) (2002) 89-105.

[30] I. Ardelean, Semiconduction in xFe2O3.(1-x)[3B2O3. PbO] glasses, Solid State Communications 27(7) (1978) 697-703.

[31] A.E. Harby, A.E. Hannora, M. Al-Assiri, M. El-Desoky, Correlation between grain size and transport properties of lead titanate based-glass–ceramic nano-composites, Journal of Materials Science: Materials in Electronics 27(8) (2016) 8446-8454.

[32] G. Greaves, Small polaron conduction in V2O5-P2O5 glasses, Journal of Non-Crystalline Solids 11(5) (1973) 427-446.

[33] A. Al-Syadi, M. Al-Assiri, H.M. Hassan, M. El-Desoky, Grain size effects on the transport properties of Li3V2(PO4)3 glass–ceramic nanocomposites for lithium cathode batteries, Journal of Materials Science: Materials in Electronics 27(4) (2016) 4074-4083.

**Table 1** Composition and physical properties of glass samples.

| **Code** | **Nominal composition (mol%)** | **ρ ±0.01 ($g/cm^3$)** | **Vm ±0.1 ($cm^3/mol$)** | **N × $10^{22}$ ($cm^{-3}$)** | **R (nm)** | **$\theta_D$ ±1 (K)** | **W ±0.01 (eV)** | **lnσ ±0.01 (S/m) (333K)** | **C** | **$\nu_0$ ±0.01(× $10^{13}$ Hz)** |
|---|---|---|---|---|---|---|---|---|---|---|
| BFO | $70Bi_2O_3$-$30Fe_2O_3$ | 7.6 | 49.2 | 1.72 | 0.387 | 740 | 0.662 | -16.40 | 0.242 | 1.54 |
| BBFO | $60Bi_2O_3$-10BaO-$30Fe_2O_3$ | 6.4 | 53.6 | 1.45 | 0.410 | 735 | 0.569 | -15.27 | 0.259 | 1.53 |
| BSFO | $60Bi_2O_3$-10SrO-$30Fe_2O_3$ | 5.9 | 57.3 | 1.33 | 0.421 | 676 | 0.355 | -10.35 | 0.357 | 1.41 |
| BCFO | $60Bi_2O_3$-10CaO-$30Fe_2O_3$ | 5.6 | 59.5 | 1.27 | 0.429 | 727 | 0.562 | -14.97 | 0.319 | 1.51 |

**Table 2 Small polaron hopping parameters of glass samples.**

| Code | $r_p$ (nm) | $N(E_F)$ ($\times 10^{21} eV^{-1} cm^{-3}$) | $\gamma_p$ ±0.01 |
|---|---|---|---|
| BFO | 0.1561 | 6.20 | 17.28 |
| BBFO | 0.1653 | 6.08 | 15.08 |
| BSFO | 0.1699 | 8.98 | 10.25 |
| BCFO | 0.1728 | 5.38 | 14 |

**Table 3 Hopping carrier mobility and density of glass samples at 333 K.**

| Code | μ ±0.2 ($cm^2 V^{-1} s^{-1}$) | $N_c$ ±0.01 ($\times 10^{17} cm^{-3}$) |
|---|---|---|
| BFO | $4.65 \times 10^{-7}$ | 10.009 |
| BBFO | $1.50 \times 10^{-4}$ | 0.097 |
| BSFO | $4.11 \times 10^{-3}$ | 0.487 |
| BCFO | $6.86 \times 10^{-4}$ | 0.029 |

**Table 4 Parameters for Greaves variable—range hopping conduction for glass samples.**

| Code | A ±0.1 ($\Omega^{-1} m^{-1} K^{1/2}$) | B ±0.2 ($K^{1/4}$) | α ±0.01 ($Å^{-1}$) |
|---|---|---|---|
| BFO | 36.85 | 210.54 | 3.78 |
| BBFO | 48.46 | 258.13 | 4.93 |
| BSFO | 50.53 | 248.30 | 5.33 |
| BCFO | 36.72 | 206.44 | 3.51 |

**Figure captions**

Fig. 1. Room-temperature XRD for the glass samples.

Fig. 2 DSC for BFO glass.

Fig. 3 Density and molar volume for the glass samples.

Fig. 4 Seebeck coefficient versus T for the glass samples.

Fig. 5 The dc conductivity (ln σ) versus inverse temperature ($T^{-1}$) for the glass samples.

Fig. 6 dc conductivity (ln σ) versus activation energy (W) at fixed temperature (333 K) for the glass samples.

Fig. 7 Effect of activation energy (W) on dc conductivity (lnσ) at fixed temperature (333K) for the glass samples.

Fig. 8 Relation between ln ($\sigma T^{1/2}$) and $T^{-1/4}$ for the glass samples.

**Figures**

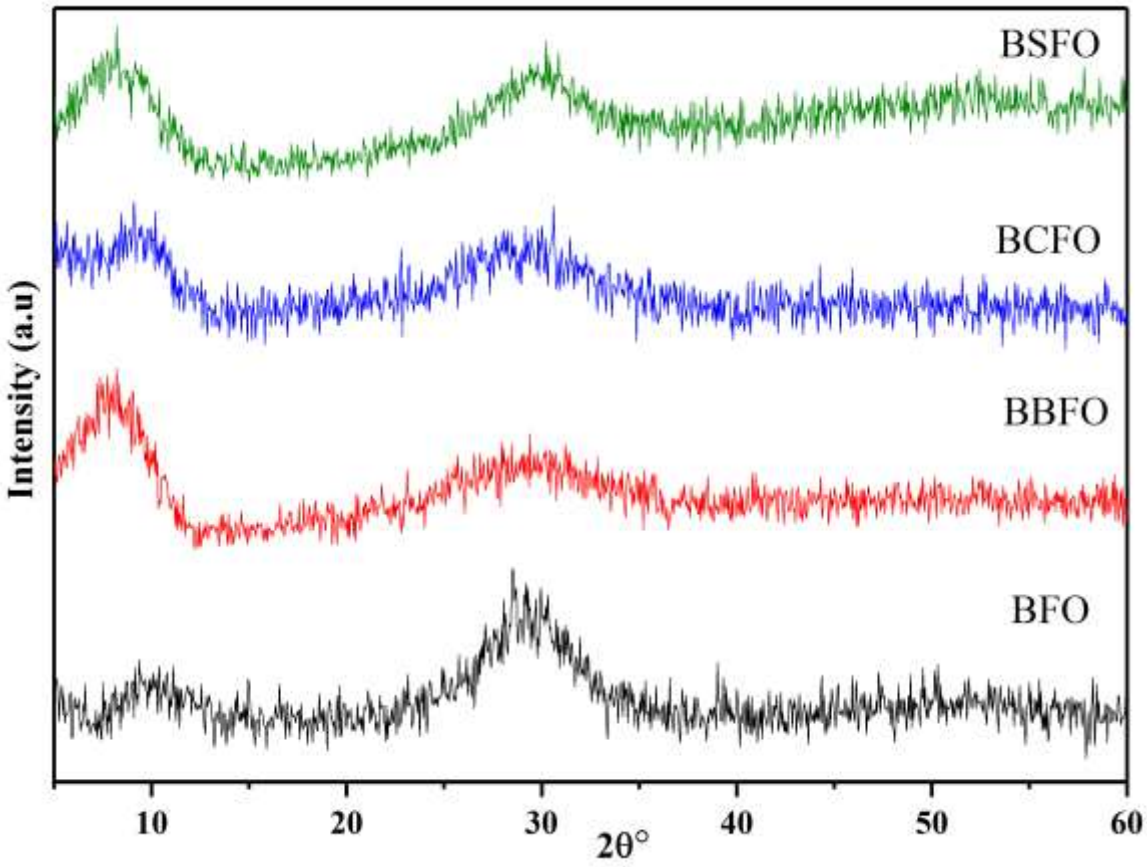


Figure 1

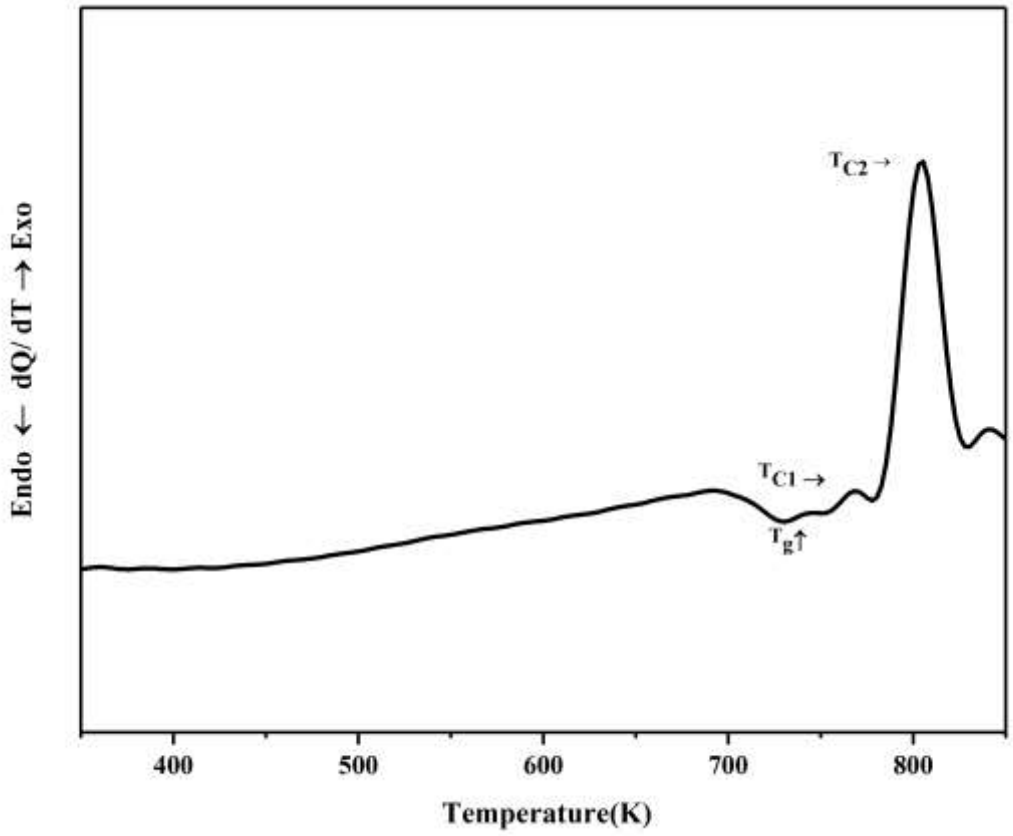


Figure 2

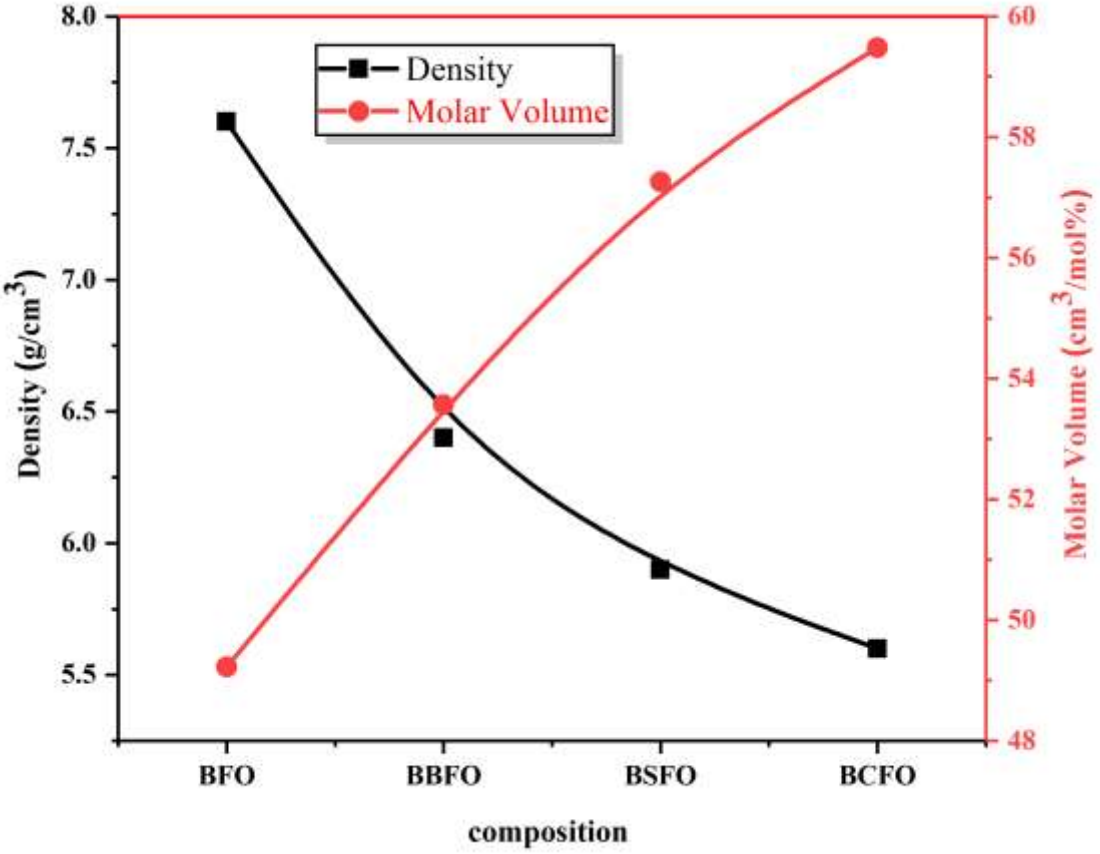
Density
Molar Volume
Density (g/cm3)
Molar Volume (cm3/mol%)
8.0
7.5
7.0
6.5
6.0
5.5
60
58
56
54
52
50
48
BFO
BBFO
BSFO
BCFO
composition

Figure 3

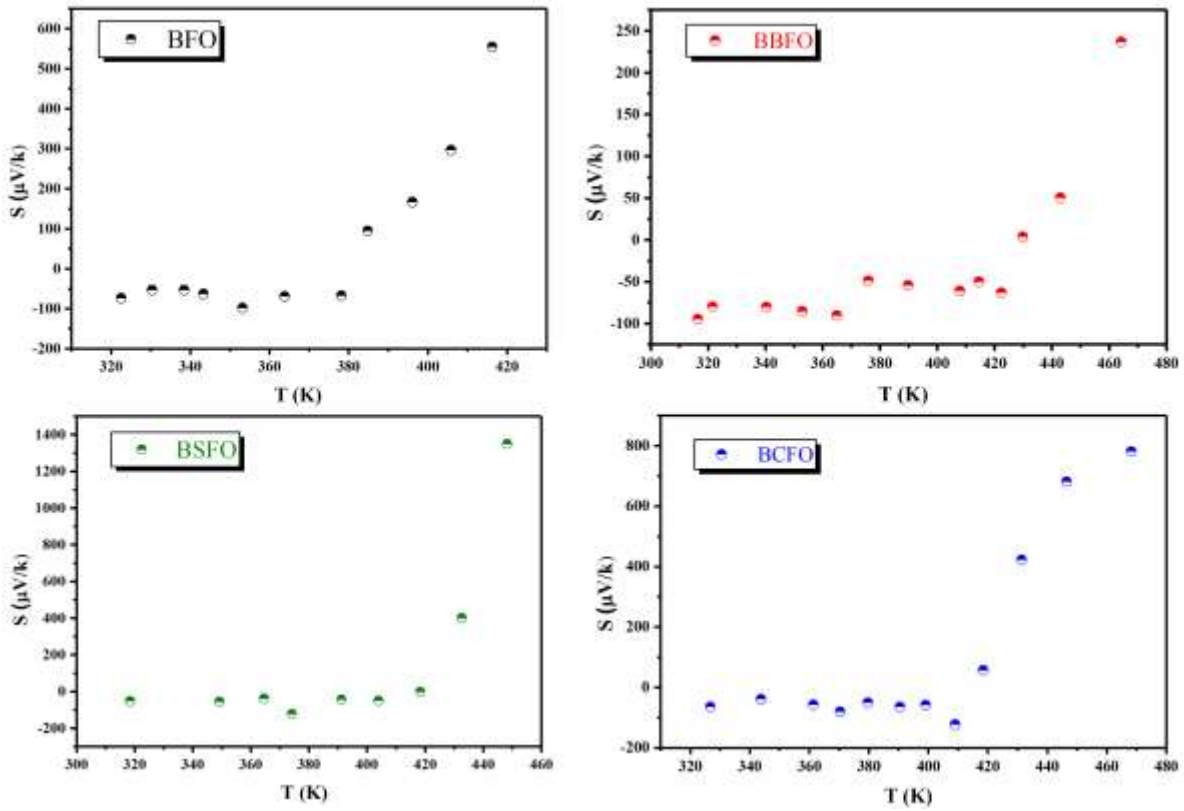


Figure 4

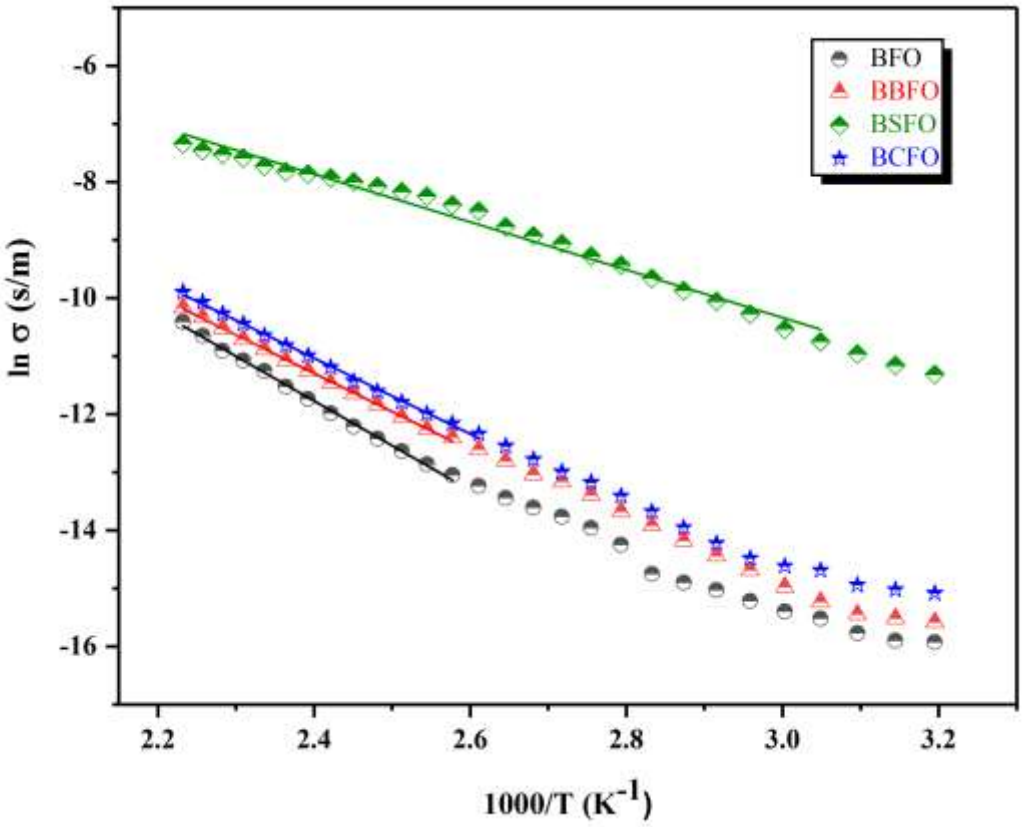


Figure 5

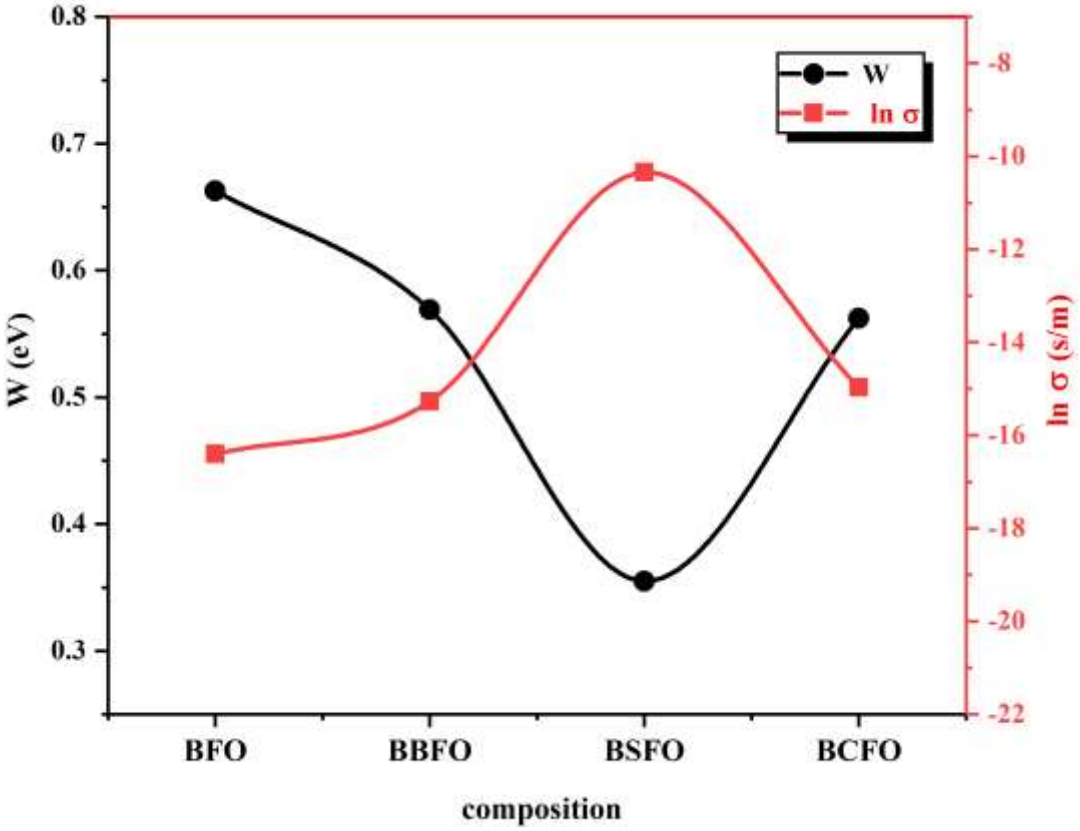
W
ln σ
W (eV)
ln σ (s/m)
0.8
0.7
0.6
0.5
0.4
0.3
-8
-10
-12
-14
-16
-18
-20
-22
BFO
BBFO
BSFO
BCFO
composition

Figure 6

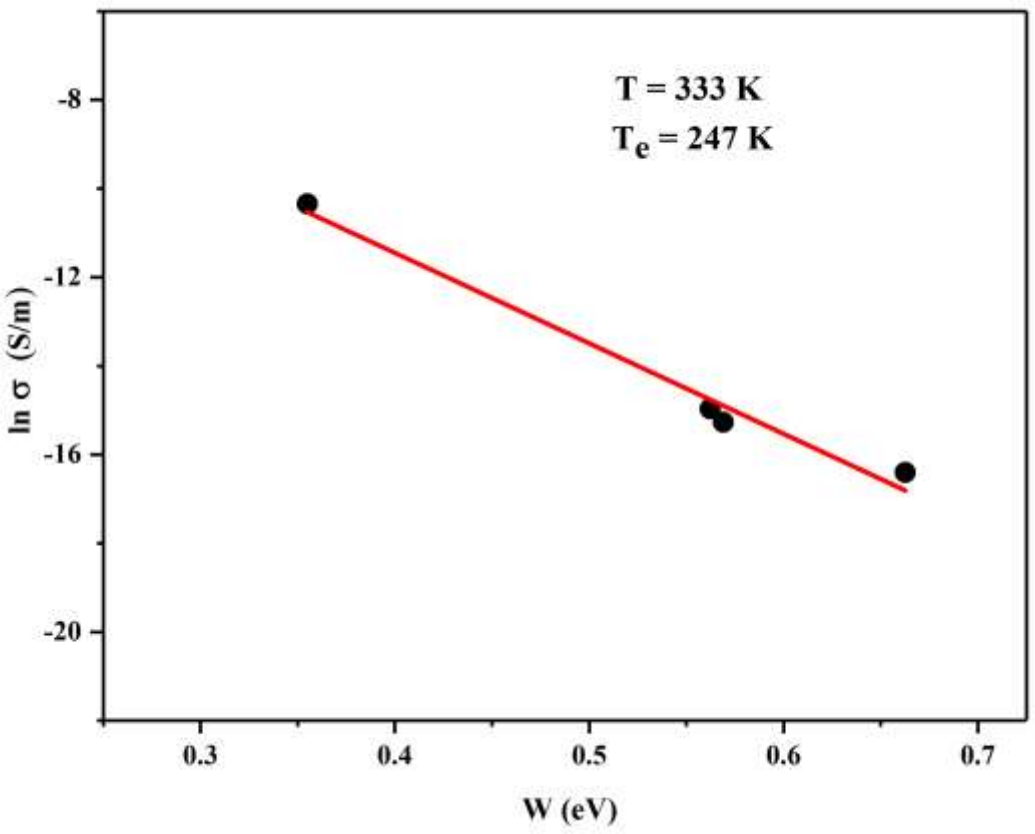


Figure 7

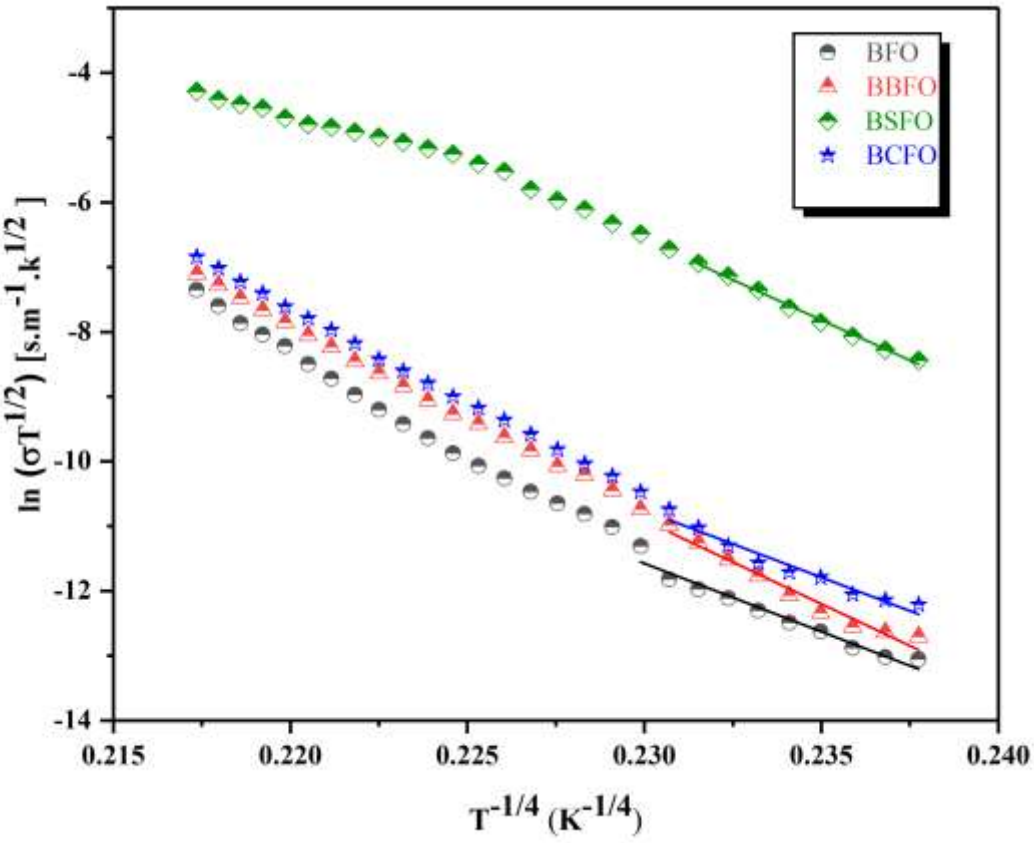
BFO
BBFO
BSFO
BCFO
-4
-6
-8
-10
-12
-14
0.215
0.220
0.225
0.230
0.235
0.240
ln (σT^1/2) [s.m^-1.k^1/2]
T^-1/4 (K^-1/4)

Figure 8

# Figures

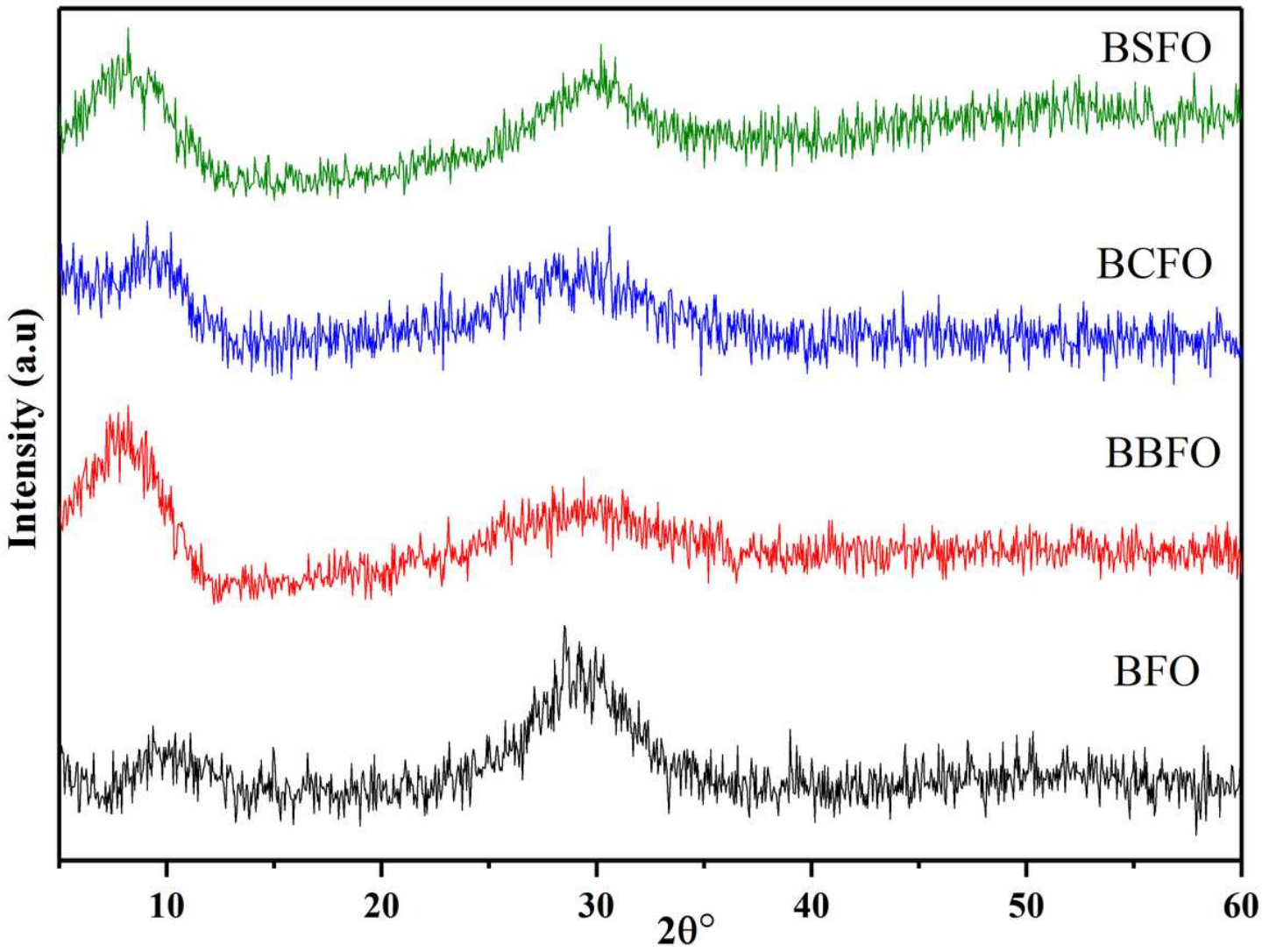


**Figure 1**

Room-temperature XRD for the glass samples.

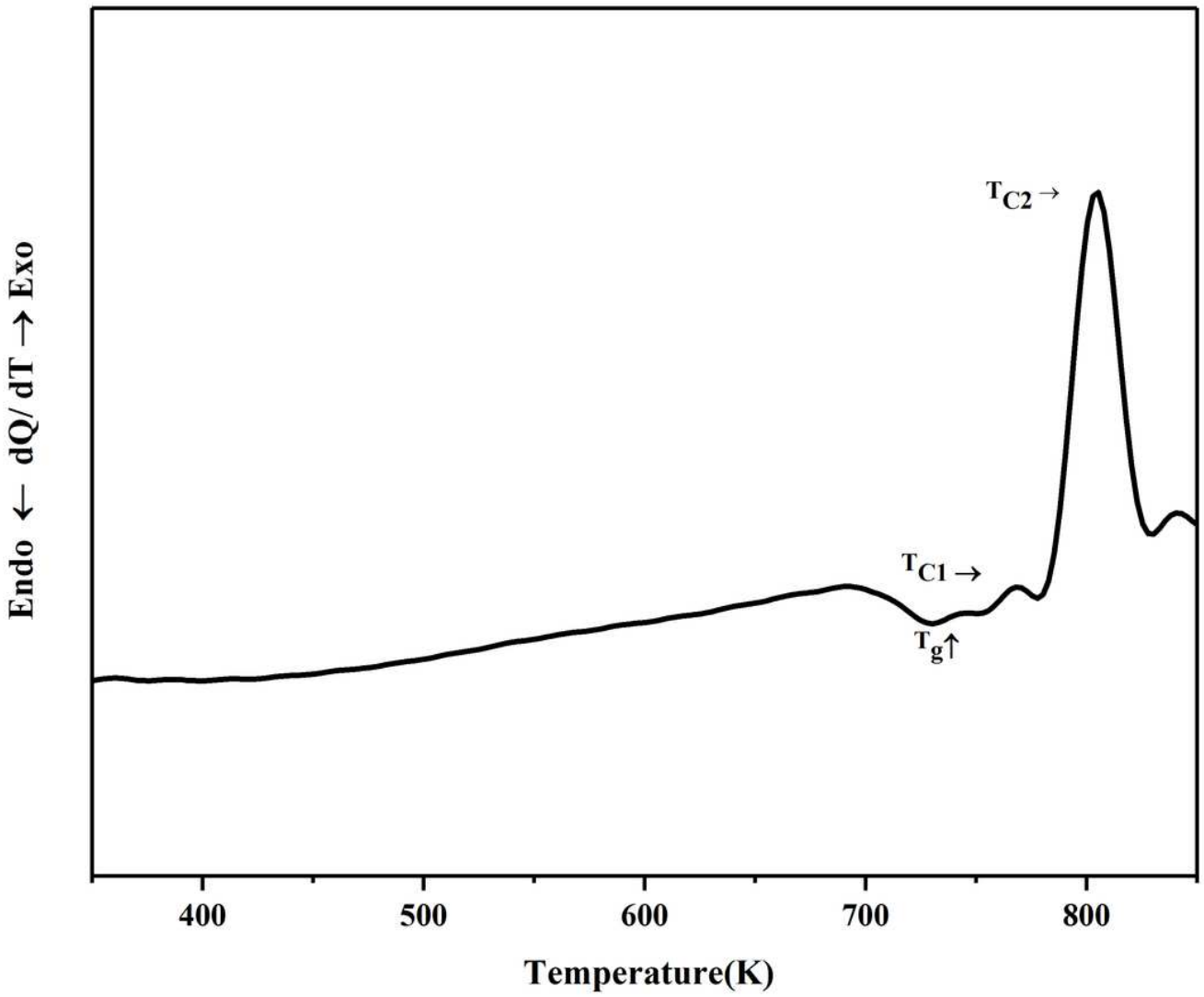


Figure 2

DSC for BFO glass.

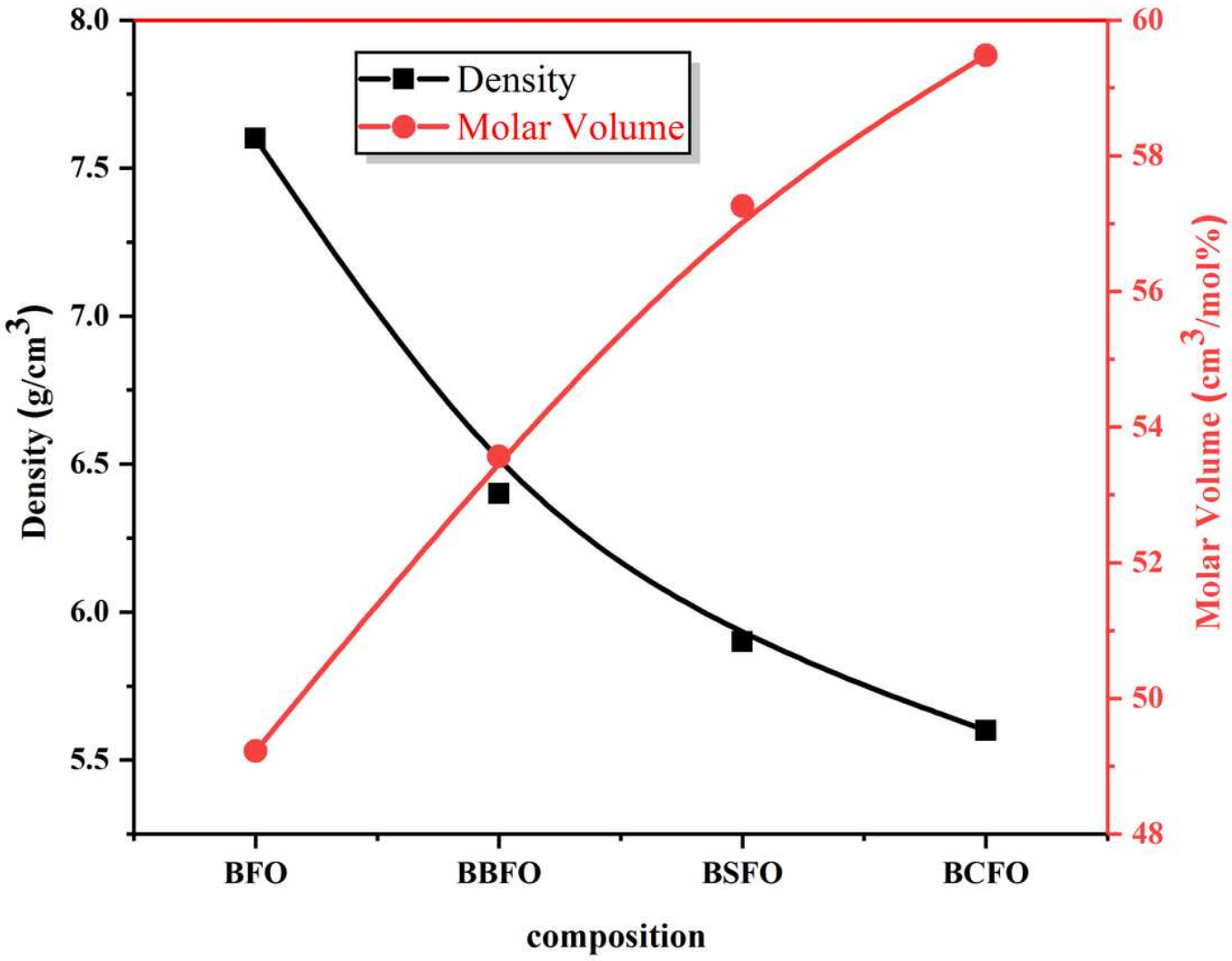


**Figure 3**

Density and molar volume for the glass samples.

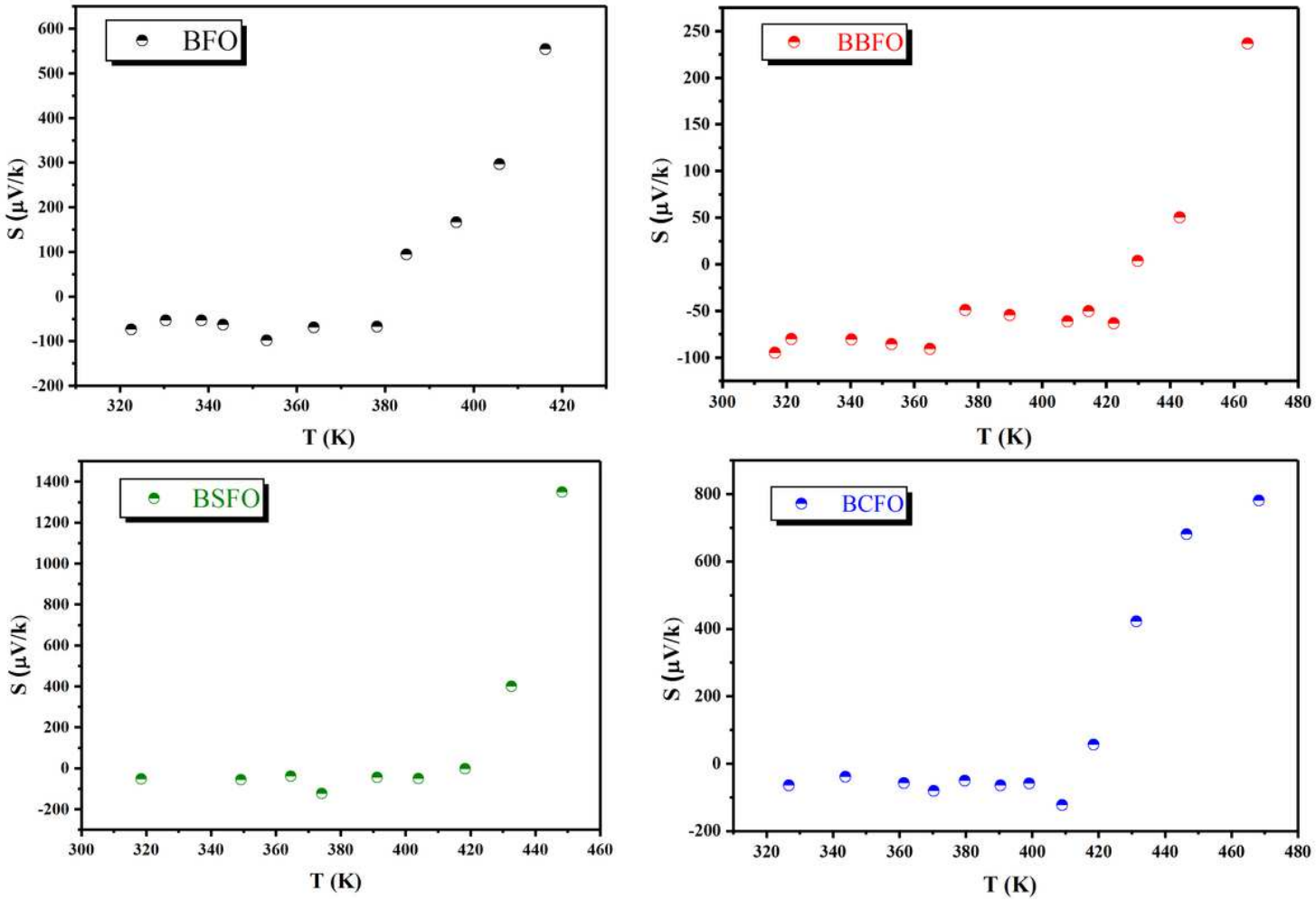


## Figure 4

Seebeck coefficient versus T for the glass samples.

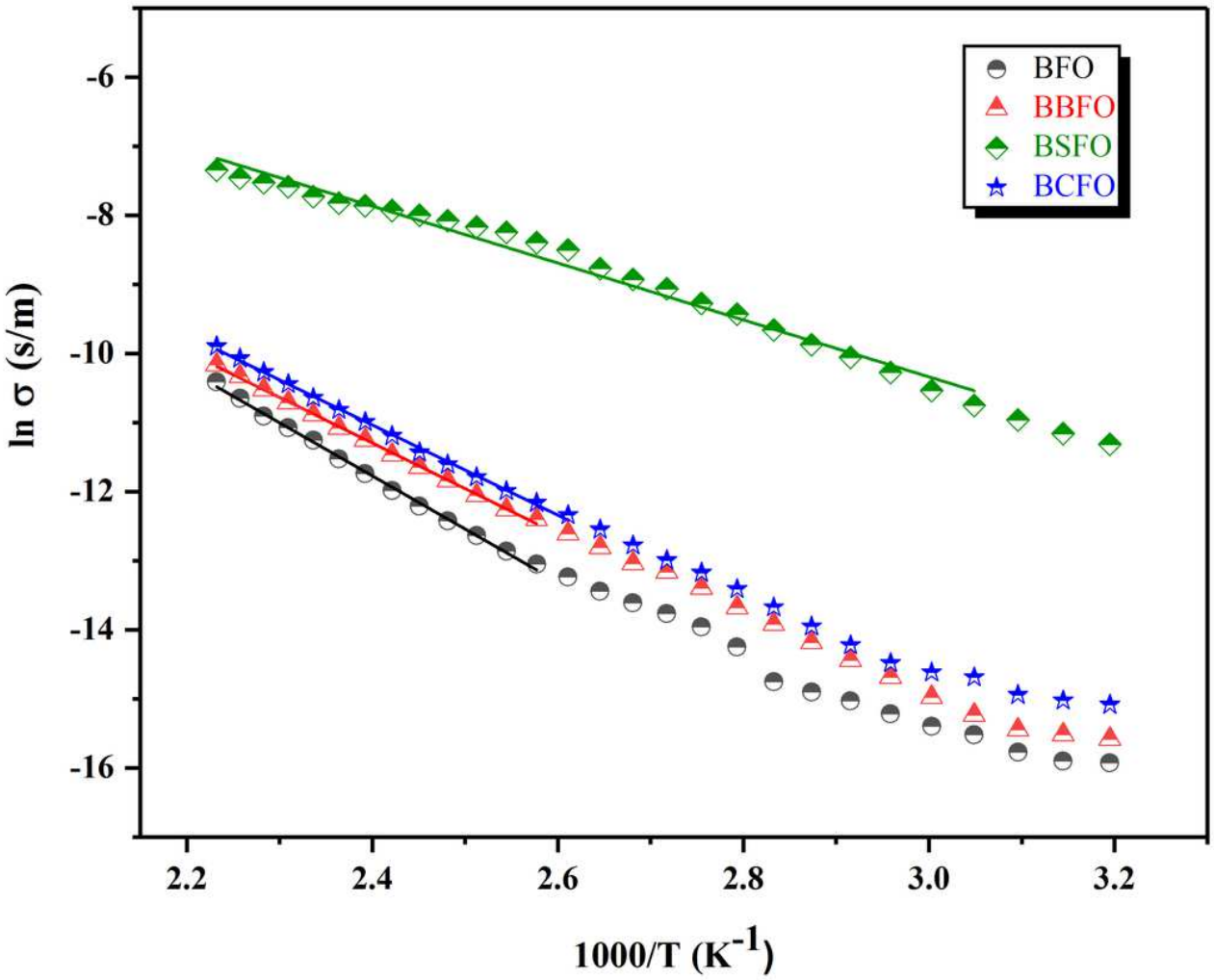


**Figure 5**

The dc conductivity (ln σ) versus inverse temperature (T-1) for the glass samples.

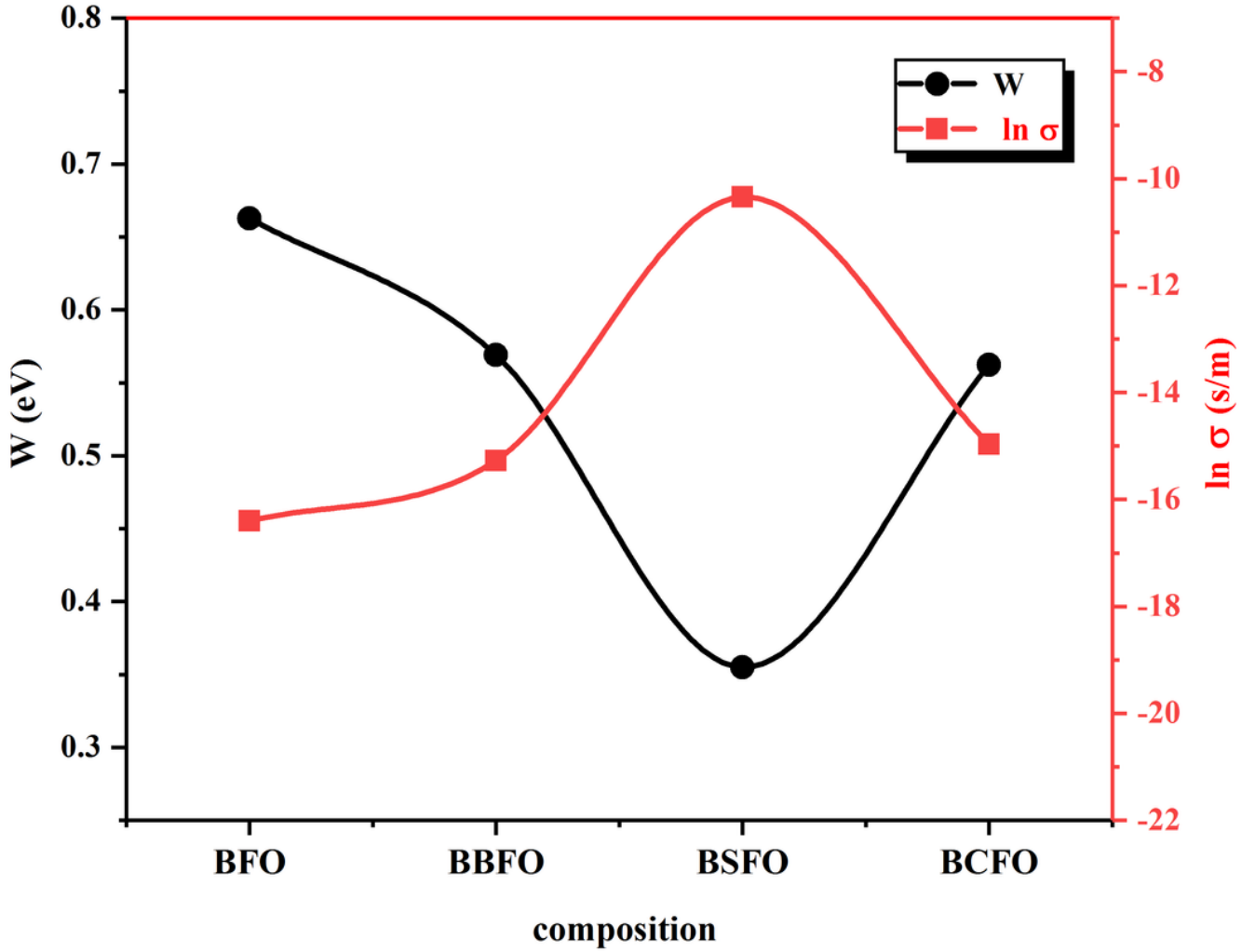


Figure 6

dc conductivity (ln σ) versus activation energy (W) at fixed temperature (333 K) for the glass samples.

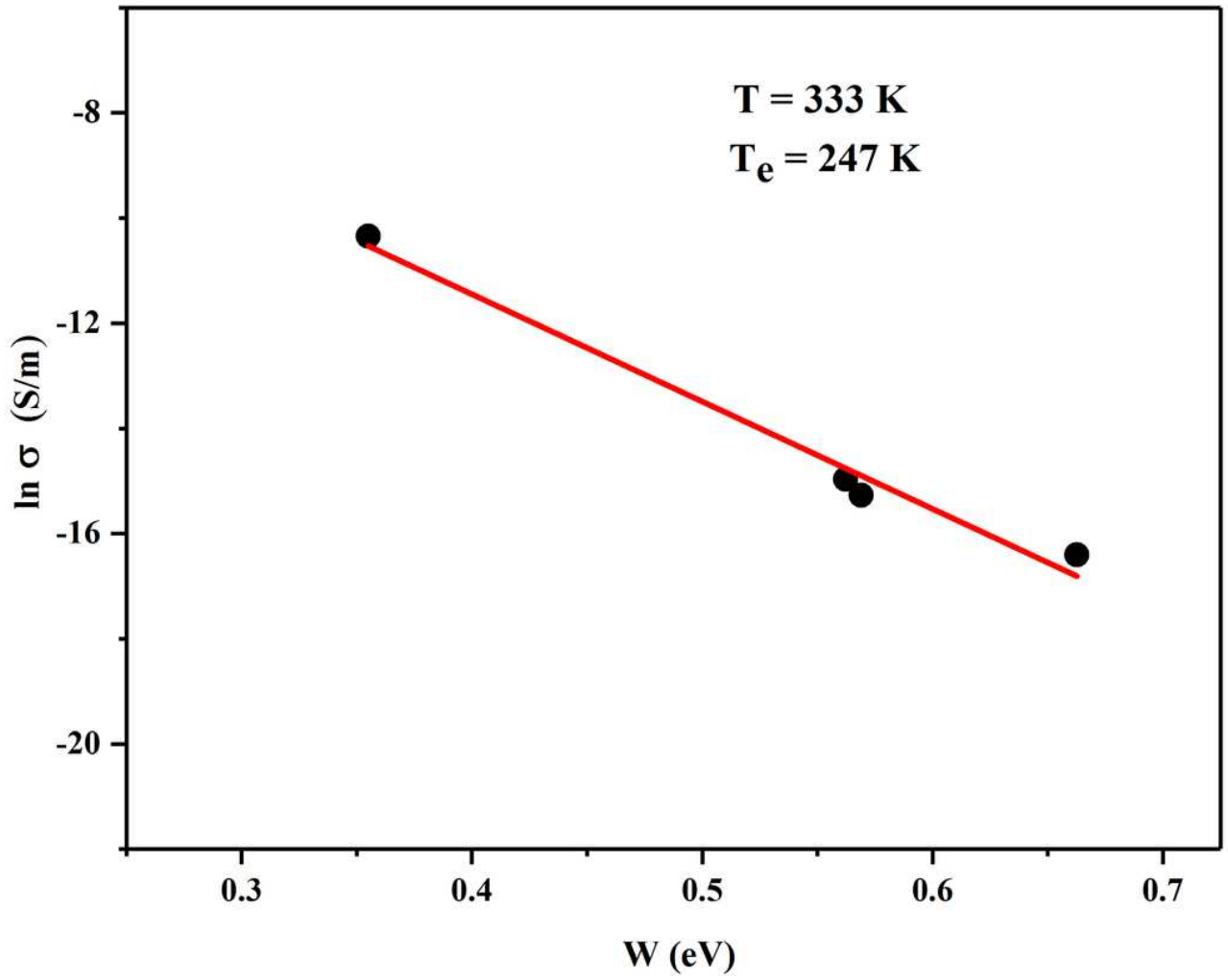


**Figure 7**

Effect of activation energy (W) on dc conductivity (lnσ) at fixed temperature (333K) for the glass samples.

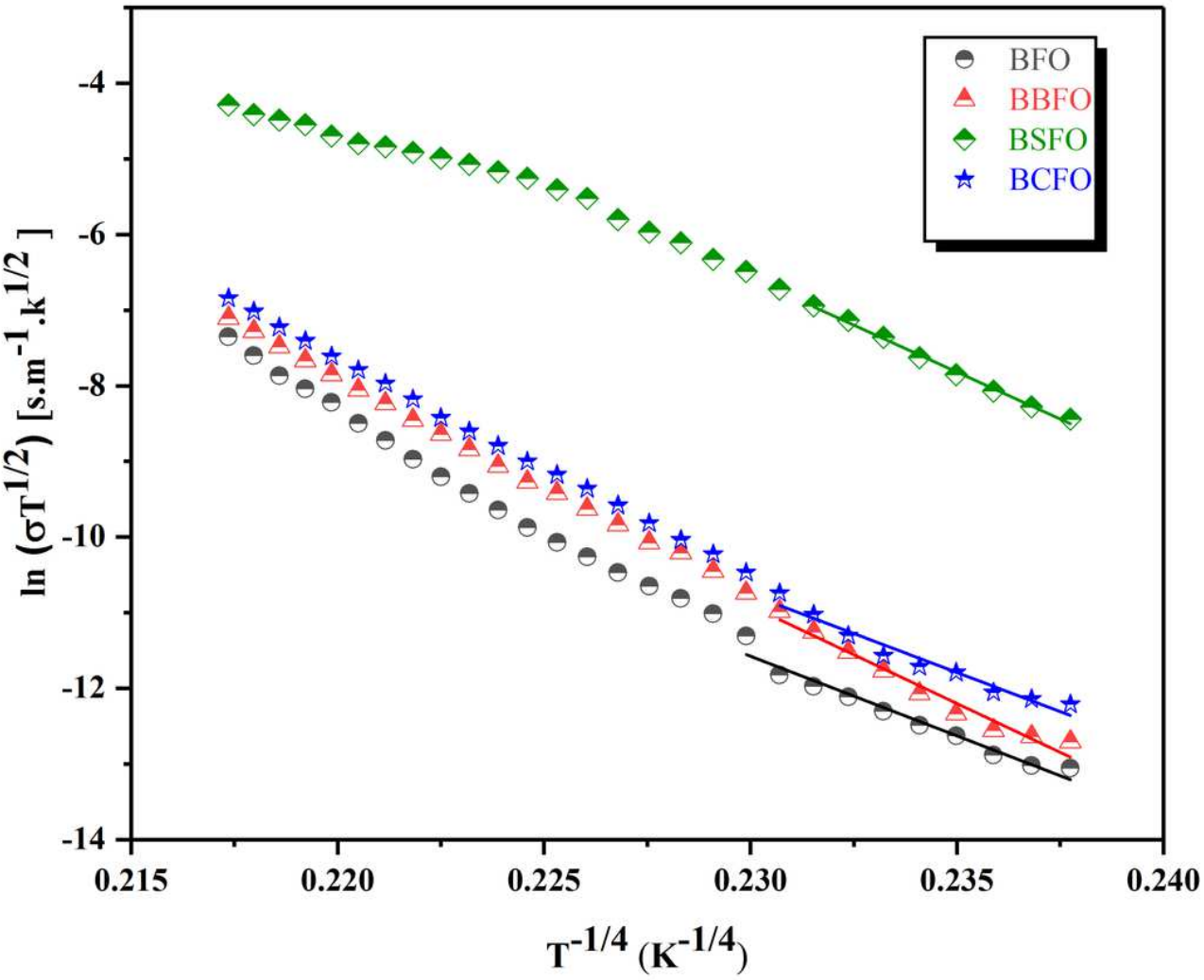


**Figure 8**

Relation between ln (σT1/2) and T -1/4 for the glass samples.